# Characterization and Modeling of a Positive Acting Chemically Amplified Resist

John S. Petersen, Chris A. Mack, James W. Thackeray, Roger Sinta, Theodore H. Fedynyshyn, J. Michael Mori, Jeffrey D. Byers and Daniel A. Miller

JSP (Shipley Company), DAM, SEMATECH, 2706 Montopolis Drive, Austin, TX, 78741-6499; CAM, FINLE Technologies, Inc., P. O. Box 162712, Austin, TX 78716; JWT, RS, TF, JMM, Shipley Company, 455 Forest Street, Marlborough, MA, 01752

## 1. ABSTRACT

Improvements in modeling of chemically amplified resists are necessary to increase the capability of doing "What if" simulations and to help interpret experimental data. One method to minimize the difference between modeled and experimental results is to use an underlying database of experimentally determined bulk dissolution rates as the source of the input parameters for the imaging engine of the lithographic model. In this paper, a R(E,z) to R(m,z) converter is discussed. The converter takes into account the amplification factor, kinetic effects and acid loss. The underlying data consist of a positive acting chemically amplified resist, XP-9402, that was processed using various post exposure bake conditions. With conversion to R(m,z), the energy of activation and Arrhenius coefficient for both the deprotection reaction and acid loss, the rate of photoacid formation, C, the chemical amplification factor for a given thermal dose and the ratio of deprotection rate constant to acid loss rate constant can be determined. These parameters are then used in the lithographic simulator PROLITH/2 version 4.1a. Results are used to understand lithographic results for photoresist that had been processed at different temperatures.

Keywords: Lithography simulator, chemically amplified resist, modeling parameters, Arrhenius Equation, dissolution rate, dissolution rate monitor, DUV or Deep Ultraviolet Photolithography

## 2. INTRODUCTION

Delineating micro-circuitry in a controllable fashion is the result of minimizing sources of process variation related to producing the circuit image in a resist material, and the transference of that image into the underlying substrate. Minimizing the sources of variation is an expensive and time consuming process. Improvements in lithographic modeling are making it possible to do some of this process definition and optimization with a minimal amount of live experiments. Using these models to do "What if" experiments during lithographic process design are helping to interpret experimental data and to solve processing problems.

The need for good modeling capabilities is especially true for chemically amplified resists. With these resists, during exposure one photo event generates one acid which, in turn, leads



Downloaded From: http://proceedings.spiedigitallibrary.org/ on 06/02/2014 Terms of Use: http://spiedl.org/terms

to many subsequent, thermally activated catalytic reactions of the acid with the polymer during the post exposure bake, PEB. Chemical changes within a resist during the various stages of the lithographic process are difficult to take into account. For this reason modeling parameters that are available for the simulators are often inaccurate and create large differences in predicted and actual results. One method to reduce the difference between modeled and experimental results is to use an underlying data base of bulk dissolution rates as the source of the input parameters for the imaging engine of the lithographic model. These data are generated by measuring the dissolution of resist under varying degrees of exposure and thermal dose. The usefulness of this approach is limited to the scope of the experimental data and the underlying assumptions made for the exposure and thermal dose. The data can not be used to do "What ifs..." for anything beyond the experimental data. Generalizing these data from a rate function for a given resist thickness and exposure, R(E,z), to a generalized function for effective extent of amplification, R(m,z), makes the original experimental data more useable.

In this paper, a R(E,z) to R(m,z) converter is discussed. The converter takes into account the amplification factor, kinetic effects and acid loss. The underlying data consist of a positive acting chemically amplified resist that was processed using various post exposure bake times and temperatures.

Once the R(m,z) conversion is made, the extracted modeling parameters will be used to interpret observed lithographic behavior of a chemically amplified resist. Of key interest is the apparent divergence of imaging results and resist contrast as the thermal dose is increased; where resist contrast is defined as the slope of the ln(develop rate) versus ln(Exposure Dose) curve. In this work the resist contrast improved with increasing post exposure bake temperature and increasing PEB times. This was due to increases in the maximum dissolution rate of completely exposed resist. Lithography, also, improved with these increases, until the PEB temperature exceeded the $T_g$ of the resist, then the imaging capability degraded significantly.

## 3. DEVELOPMENT OF R(E,z) CONVERTER

The R(E,z) to R(m,z) converter used in this work is shown in equation 1 and is derived afterwards:

$$m = e^{-k_{amp} \cdot \left(1-e^{-C \cdot dose}\right) \cdot \frac{(1.0-e^{-k_{loss} \cdot t})}{k_{loss}}} \quad (1)$$

In this equation, m is the normalized concentration of unreacted blocking sites, $[M]_t$; $k_{amp}$ is the temperature dependent rate of deprotection of the blocked resin for PEB time, t; C is the rate of acid generation with exposure dose, dose; and $k_{loss}$ is the temperature dependent rate of acid loss during the PEB. Equation 1 is derived in the next sections.



Downloaded From: http://proceedings.spiedigitallibrary.org/ on 06/02/2014 Terms of Use: http://spiedl.org/terms

## 3.1. Exposure

First a single acid is generated in catalytic resists by conversion of a photo acid generator, PAG, during exposure to actinic light at some intensity, I(h$\upsilon$):

$$PAG + I(h\upsilon) \xrightarrow{C} Acid \quad (2)$$

and has been described by

$$\frac{d[PAG]}{dt'} = -C \cdot [PAG] \cdot I \quad (3)$$

where $t'$ is the exposure time. Rearranging equation 3 and integrating with respect to exposure time yields:

$$[PAG]_t = [PAG]_0 \cdot e^{-C \cdot I \cdot t'} \quad (4)$$

where $dose \equiv I \cdot t'$ and $[PAG]_0$ is the initial concentration of photo acid generator. Now the concentration of acid for a particular exposure dose is described as:

$$[PAG]_{dose} = [PAG]_0 \cdot e^{-C \cdot dose} \quad (5)$$

To then solve for $[Acid]_{dose}$, subtract the $[PAG]_{dose}$ from $[PAG]_0$,

$$[Acid]_{dose} = [PAG]_0 - [PAG]_{dose} \quad (6)$$

then substitute into this equation into equation 5 to give the concentration of acid at any given dose, shown in Equation 7

$$[Acid]_{dose} = [PAG]_0 \left(1 - e^{-C \cdot dose}\right) \quad (7).$$

## 3.2. Deprotection and Acid loss

After formation of the acid during exposure, the resist is baked. During this step the thermal assisted acid catalytic deprotection of the polymer occurs. This deprotection of the polymer in the exposed areas makes the photo resist soluble in aqueous base. In this work the reaction is assumed to follow a first order irreversible reaction.

$$Acid + M \xrightarrow{k_{amp}} Acid + X \quad (8)$$



Downloaded From: http://proceedings.spiedigitallibrary.org/ on 06/02/2014 Terms of Use: http://spiedl.org/terms

where M are the protecting moieties on the polymer and X is the products of the deprotection reaction. The reaction is catalytic, so for every acid consumed an acid is formed for subsequent reaction. This reaction proceeds until the acid is consumed by a competing reaction or by loss to the environment and this loss is generically expressed as.

$$\text{Acid} \xrightarrow{k_{loss}} \qquad (9)$$

with the rate of loss defined as $k_{loss}$. The quenching reaction can be with any material that is more basic than the Acid. This includes the products of the deprotection reactions, the unreacted portion of the polymer, other components of the resist system, the substrate or bases absorbed from the environment.

Mathematically, the acid concentration, [Acid] is described as

$$\frac{d[Acid]}{dt} = -k_{loss} \cdot [Acid] + \nabla\left(D_{acid} \cdot \nabla[Acid]\right) \qquad (10)$$

$\nabla D$ is three dimensional Fickian diffusion of the acid within the resist film and $\nabla[Acid]$ is the concentration gradient of acid in the film as a result of changing exposure conditions in the film caused both by internal interference of light and absorbance of light by the resist film during exposure and the aerial image. For the derivation of the R(E,z) converter, diffusion has been ignored for the moment by using dissolution rates from one thickness, z=300nm into the film, and assuming because of a constant exposure condition that the local gradient in [Acid] is zero.

$$\nabla[\text{Acid}] \approx 0 \qquad (11)$$

This assumption in reality is not a good one but will later be accounted for during subsequent reiteration using parameters derived from the R(E,z) converter with modeling of diffusion using PROLITH/2 version 4.1a.

Now, with Acid changes due to diffusion out of the way for the moment, acid loss during the PEB can be solved in a straight forward fashion. First, assuming first order kinetics, describe the change in [Acid] with respect to time

$$\frac{d[\text{Acid}]}{dt} = -k_{loss} \cdot [\text{Acid}] \qquad (12)$$

Combine like terms, integrate with respect to PEB time, t, and solve for the time dependent concentration of Acid, $[\text{Acid}]_t$

$$[\text{Acid}]_t = [\text{Acid}]_{dose} \cdot e^{-k_{loss} \cdot t} \qquad (13)$$



Downloaded From: http://proceedings.spiedigitallibrary.org/ on 06/02/2014 Terms of Use: http://spiedl.org/terms

Substitute Equation 7 into Equation 13

$$[\mathrm{Acid}]_t = [\mathrm{PAG}]_0 \cdot \left(1 - e^{-C \cdot \mathrm{dose}}\right) e^{-k_{loss} \cdot t} \quad (14).$$

Equation 14 can now be used to solve for the concentration of [M] at any time t during the PEB. This is determined by the rate of reaction at the PEB temperature and is assumed to be first order in [Acid] and in [M] and is expressed as

$$\frac{d[M]}{dt} = -k_{amp} \cdot [Acid] \cdot [M] \quad (15)$$

Then after rearranging and replacing [Acid] with $[\mathrm{Acid}]_t$, treating exposure generated [Acid] as a constant, integrating with respect PEB time as shown in equations 16, 17, 18

$$\int_0^t \frac{d[M]}{[M]} = \int_0^t -k_{amp} \cdot [Acid]_t \cdot dt \quad (16)$$

$$\int_0^t \frac{d[M]}{[M]} = \int_0^t -k_{amp} \cdot [\mathrm{PAG}]_0 \cdot \left(1 - e^{-C \cdot dose}\right) \cdot e^{-k_{loss} \cdot t} \cdot dt \quad (17)$$

$$\int_0^t \frac{d[M]}{[M]} = -k_{amp} \cdot [\mathrm{PAG}]_0 \cdot \left(1 - e^{-C \cdot dose}\right) \cdot \int_0^t e^{-k_{loss} \cdot t} \cdot dt \quad (18)$$

to yield

$$\ln\left(\frac{[\mathrm{M}]_t}{[\mathrm{M}]_0}\right) = -k_{amp} \cdot [\mathrm{PAG}]_0 \cdot \left(1 - e^{-C \cdot dose}\right) \cdot \frac{(1.0 - e^{-k_{loss} \cdot t})}{k_{loss}} \quad (19)$$

Equation 1 comes from taking the exponential of both sides of Equation 19 and solving.

$$m = e^{-k_{amp} \cdot \left(1 - e^{-C \cdot dose}\right) \cdot \frac{(1.0 - e^{-k_{loss} \cdot t})}{k_{loss}}} \quad (1)$$

m is normalized but if the actual $[\mathrm{M}]_0$ is known an exact solution can be written.



Downloaded From: http://proceedings.spiedigitallibrary.org/ on 06/02/2014 Terms of Use: http://spiedl.org/terms

(1a)

$$[M]_t = [M]_0 \, e^{-k_{amp} \cdot [PAG]_0 \cdot \left(1-e^{-C \cdot dose}\right) \cdot \frac{(1.0-e^{-k_{loss} \cdot t})}{k_{loss}}}$$

In this work we substituted the Arrenhius equations,

$$k_{amp_or_loss} = Ae^{\frac{-E_{Activation}}{RT}} \quad (20)$$

for the rate of deprotection and the rate of acid loss into Equation 1. In Equation 20, A is the Arrhenius coefficient or pre-exponential, R is the universal gas constant, 1.99 cal•mole$^{-1}$Kelvin$^{-1}$, T is the temperature in Kelvin and $E_{Activation}$ is the activation energy of the respective reaction.

## 4. Experimental

To generate the dissolution rate data 100mm wafers were coated with Shipley XP-9402 to a post apply bake thickness of 792.5nm. This thickness is an $E_{MIN}$ thickness on the swing curve. For this experiment a 115°C/90s post apply bake was used for all wafers. After curing the resist, the wafers were exposed with twenty-one different bulk areas per wafer using a 0.35NA/248nm GCA Laser Step. After exposure, the wafers were baked using various thermal doses. The PEB conditions were varied from 70 to 115C° for 30 to 120s, see Table 1. The resist was developed with Shipley MF-321 at 21°C. A Perkin Elmer multichannel DRM was used to monitor the develop rate of the resist for the different sets of exposure and thermal doses.

**Table 1: Post Exposure Bake Conditions used for the R(E,z) to R(m,z) conversion.**

| PEB Temperature (°C) | PEB Time (s) |
|---|---|
| 70 | 90 |
| 80 | 90 |
| 85 | 60, 90, 120 |
| 90 | 30, 45, 60, 75, 90, 105, 120 |
| 95 | 30, 60, 90, 120 |
| 100 | 90 |
| 105 | 90 |
| 115 | 90 |

## 5. Parameter Extraction

After collection of the rate data, instantaneous rates at a 300nm depth into the film for all post exposure bake processes were used in the R(E,z) converter, see Figure 1. Rates from a fixed depth were chosen to avoid dependence on variations in local [Acid] due to



Downloaded From: http://proceedings.spiedigitallibrary.org/ on 06/02/2014 Terms of Use: http://spiedl.org/terms

**Figure 1: Combined dissolution rate data for all post exposure bake conditions shown in Table 1. These rates are from 300nm depth from the resist surface.**

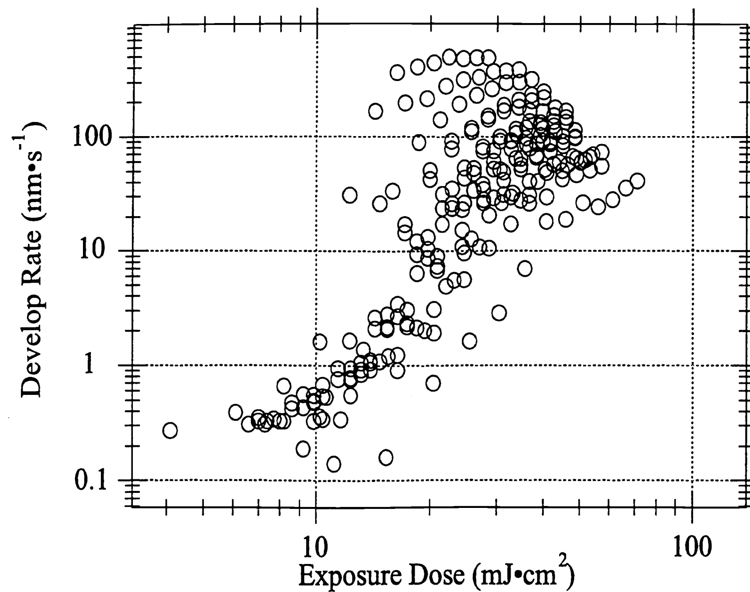


exposure level variation in the resist film from interference and absorption effects. The amplification factor, activation energies and the Arrhenius Coefficients for both deprotection and acid loss, and the ratio of $\frac{k_{amp}}{k_{loss}}$ are obtained stochastically by converting exposure dose to m using Equation 1, plotting rate versus m and looking for convergence of the rate data, adjusting the parameters and, using a half interval search technique, trying again until a good fit is found by visual inspection. In this study the C-value was not varied. Instead, based on a colormetric titration, the C-value was previously determined experimentally to be $0.035 cm^2 \cdot mJ^{-1}$ [1]

Once parameters were found that showed what appeared to be visually the best fit of the data, they were further refined by fitting the rate versus m data to Equation 21,and

results shown in Figure 2.

$$Rate = R_{MAX} \left( \frac{\frac{(n+1)(1-m_{th})^n (1-m)^n}{n-1}}{\frac{(n+1)(1-m_{th})^n}{n-1} + (1-m)^n} \right) + R_{MIN} \tag{21}$$



Downloaded From: http://proceedings.spiedigitallibrary.org/ on 06/02/2014 Terms of Use: http://spiedl.org/terms

In this equation, $R_{MAX}$ and $R_{MIN}$ are, respectively, the maximum and minimum

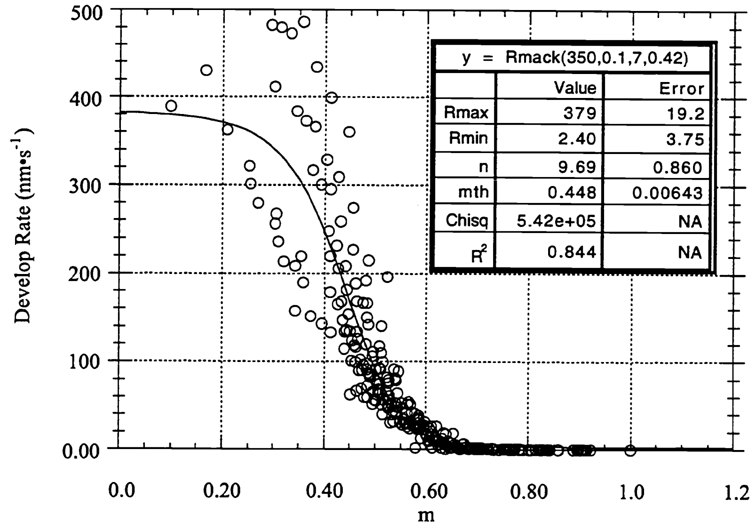


**Figure 2: Rate versus m, converted from Rate versus exposure dose shown in Figure 1.**

development rates in nm•s$^{-1}$; $n$ is the developer selectivity of the resist; and $m_{th}$ is the normalized threshold concentration of protected sites on the polymer.

## 6. Results and Discussion

The parameters from the first attempts at R(E,z) to R(m,z) conversion of the data set shown in Figure 1 yielded fits to equation 21 of $0.8 \leq R^2 \leq 0.9$. Figure 2 contains the results of a representative fit for the entire data set, it had an $R^2=0.84$. Examination of the residuals show a lack of randomness in the data sets. This systematic error means that there are phenomena that the converter does not describe adequately or that there is experimental bias within the data sets, or both. Phenomenological sources of error are caused by not adequately accounting for the effect of changes in the resist that occur from exposure to both radiant and thermal energy. These changes can affect the rates of both acid diffusion and the deprotection reaction, and dissolution of the resist during development, thus causing a discrepancy in the predicted results from the actual. Experimentally, an example of systematic error from bias is a discrepancy in the recorded post exposure bake process and the actual thermal history the wafer experiences in the catalytically active portion of the post exposure bake process. This is because both the time and the integrated temperature, from warm-up to cool down, does not match the recorded process. Total accounting of all the data with the R(E,z) converter is beyond the scope of this work and is an ongoing effort. However, using the current model and looking at individual post exposure bake process of the full data sets it is possible to



Downloaded From: http://proceedings.spiedigitallibrary.org/ on 06/02/2014 Terms of Use: http://spiedl.org/terms

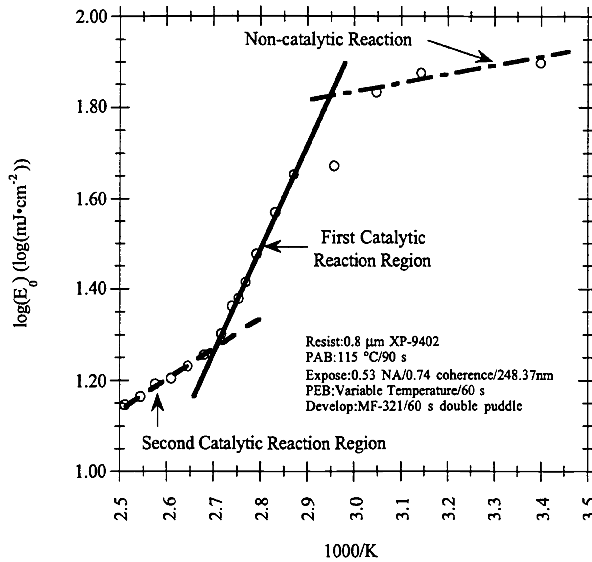


**Figure 3: Pseudo-Arrhenius data for XP-9402(Ref 3).**

ascertain where error in the data set exists and to provide a pathway to understanding what needs to be done to improve the converter.

To begin this examination and refinement, a review of the minimum exposure dose, $E_0$, required to dissolve 100% of the resist for a fixed set of processing conditions as a response to post exposure bake temperature for the XP-9402 will be discussed. Previously it had been shown that XP-9402 has three distinct mechanisms involved in its dissolution behavior.[2] Figure 3, is a pseudo-Arrhenius plot of $\log(E_0)$ versus 1000/Kelvin which is used to show at which post exposure bake temperature range each mechanism dominates. Each linear region on the graph is indicative of a dominant reaction mechanism within its respective temperature range. Figure 3 shows distinct temperature regions of linearity, suggesting three different mechanisms that dominate the $E_0$ behavior of the resist. First there is a low temperature, non-catalytic region, from room temperature to around 75°C post exposure bake. In this region, the unexposed PAG acts as an inhibitor and the exposed PAG acts as a dissolution rate accelerator. The second region, between 75°C and 90°C is a kinetically controlled catalytic region. The third region, from 100°C to ≥125°C is a diffusion controlled catalytic region. The 95°C post exposure bake, near the inflection between the two catalytic regions, exhibits characteristics of both catalytic regions.

Similarly, as shown in Figure 4, examination of the lack of fit in the R(E,z) data analysis shows that the model does not explain these different mechanistic regions in the conversion to R(m,z). In this Figure, there is a large spread in the data set, especially in the low m-value, high dose, areas of the graph. Analysis of the individual components



Downloaded From: http://proceedings.spiedigitallibrary.org/ on 06/02/2014 Terms of Use: http://spiedl.org/terms

show four main groupings as the source of divergence in the total data set. First the 70°C for 90s post exposure bake process did not converge with any of the parameter variants examined and is consistent with region 1, low temperature inflection region in Figure 3. Next, corresponding to the kinetically controlled reaction mechanism in Figure 3, the second group of data contains the 80°C to 90°C data. The third contains the 95°C post exposure bake processes. This data in Figure 4 is from the inflection between the two catalytic regions in Figure 3. The fourth contains the 100 °C to 115°C post exposure bake, 90s processes from the diffusion controlled region in Figure 3. Since the current R(E,z) to R(m,z) converter did not capture the differences in the different temperature zones, the first refinement is to solve for each region separately.

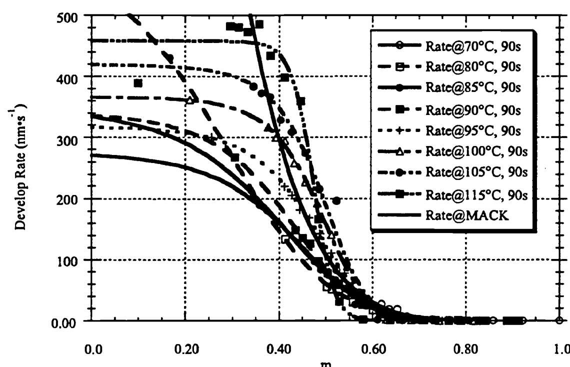


**Figure 4: Representative R(m,z) data using the set of parameters shown in Table 2. Note the deviation in the curves from the all data fit shown as the Mack curve.**

Figures 5 and 6 shows the R(m,z) data for the 80°C to 90°C and the 100°C, 105°C and 115°C post exposure bake processes, respectively.

**Figure 5: R(m,z) for the 80°C, 85°C and 90°C PEB processes using the parameters in Table 2.**

**Figure 6: R(m,z) for 100°C, 105°C and 115°C PEB processes using parameters from Table 2.**

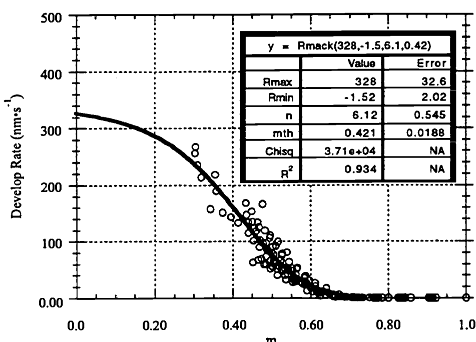


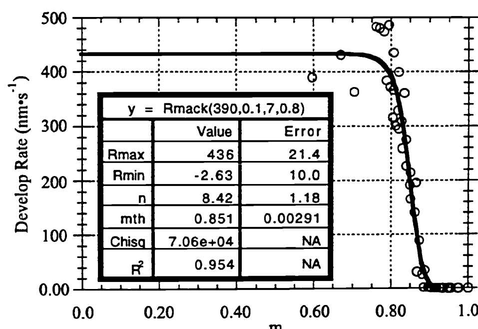




Downloaded From: http://proceedings.spiedigitallibrary.org/ on 06/02/2014 Terms of Use: http://spiedl.org/terms

**Table 2: Parameters extracted for the kinetically controlled and the diffusion controlled regions from Figure 2.**

| Dominate mechanism | All | Kinetic | Diffusion |
|---|---|---|---|
| Post Exposure Bakes | 70°C, 80°C, 85°C,90°C, 95°C, 100°C, 105°C, 115°C | 80°C, 85°C and 90°C | 100°C, 105°C and 115°C |
| $k_{amp}/k_{loss}$ | 1.2 | 1.2 | 0.4 |
| PEB Time | 90s | 90s | 90s |
| PEB Temperature | 90°C | 90°C | 105°C |
| Amplification Factor† | 5.36 | 5.36 | 8.09 |
| C | 0.035 $cm^2 \bullet mJ^{-1}$ | 0.035 $cm^2 \bullet mJ^{-1}$ | 0.035 $cm^2 \bullet mJ^{-1}$ |
| $E_{activation}$ Amplification | 7.5 | 7.5 | 7.5 |
| ln(A) Amplification | 7.57 | 7.57 | 7.57 |
| $E_{activation}$ Acid Loss | 0 | 0 | 0 |
| ln(A) Acid Loss | -3.0 | -3.0 | -1.5 |
| $R_{MAX}$ | 379(±19) $nm \bullet s^{-1}$ | 328(±33) $nm \bullet s^{-1}$ | 436(±21) $nm \bullet s^{-1}$ |
| $R_{MIN}$ | 2.4(±3.8) $nm \bullet s^{-1}$ | -1.5(±2) $nm \bullet s^{-1}$ | -2.6(±10) $nm \bullet s^{-1}$ |
| n | 9.7(±0.9) | 6.1(±0.5) | 8.4(±1) |
| mth | 0.45(±0.01) | 0.42(±0.02) | 0.85(±0.003) |
| $R^2$ | 0.84 | 0.93 | 0.95 |

† Factor based on the same activation energy and pre-exponential for both processes and the change in temperature.

In Table 2, the kinetic and diffusion controlled regions converge with the same Arrhenius values for both deprotection and acid loss. The activation energy of 0 $kcal \bullet mole^{-1}$ for acid loss suggests that the acid forms an equilibrium with some component in the resist. The amplification factor is different simply because the two sets of parameters are based on different post exposure bake processes. However, while there are similarities, these data suggest very different R(m,z) behavior. In the kinetic controlled region, the diffusion length of the acid within the resist is insufficient to diffuse across the standing wave nodes. To smooth the standing waves, PROLITH/2 version 4.1a simulations, using a reaction-diffusion model, estimates that diffusion lengths must be in the neighborhood of 100nm to 130nm. Diffusion lengths that are less than that require more exposure to clear each node. The increased exposure to clear the nodes pushes the R(m,z) curve to lower m value and lower developer selectivity because of proportionally higher exposure in the anti-nodal region of the standing waves. In the diffusion controlled region, there is no such limitation, the nodal and anti-nodal regions are sufficiently averaged, and the developer selectivity is significantly higher. Also, because of the acid gradient at the higher temperature processes, the R(m,z) curve can turn on at higher values of m.

Also, note that the apparent rate of deprotection, $k_{amp}$, and the rate of acid loss, $k_{loss}$, is different between the two catalytic regions as indicated by the ratio of the two. The



Downloaded From: http://proceedings.spiedigitallibrary.org/ on 06/02/2014 Terms of Use: http://spiedl.org/terms

activation energy for acid loss is zero and its pre-exponential is less than for deprotection. This suggests that $k_{amp} \geq k_{loss}$ instead of the reverse and that the ratio is less than one because above 90°C to 95°C post exposure bake temperature the kinetic controlled rate of deprotection is no longer the dominant mechanism and as a result is no longer a primary factor for the R(E,z) converter to converge the data.

Lithographically, besides the response to increased diffusion lengths of the acid at higher post exposure bake temperatures, the response to the two different R(m,z) curves shown in Figures 5 and 6 will be different because of which gradient of m on the diffused latent image is sampled during development. Experimentally, as shown in Figure 7, changes in post exposure bake temperature cause changes in nested to isolated line bias. Prolith

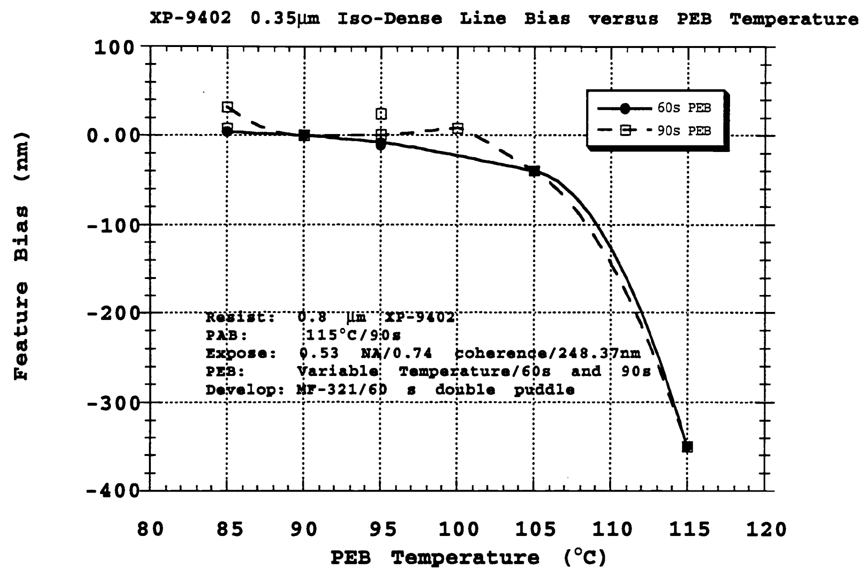


**Figure 7: Nested to isolated line bias for 350 nm features for XP-9402 with respect to different PEB temperatures.**

simulations of 350nm isolated and nested lines using a fixed diffusion length and the parameters from the kinetic and diffusion controlled regions are shown in Table 3.



**Downloaded From: http://proceedings.spiedigitallibrary.org/ on 06/02/2014 Terms of Use: http://spiedl.org/terms**

**Table 3: Comparison of simulated to experimental isolated to nested line bias for 350 nm features. A diffusion length of 130 nm is used for both sets of simulations.**

| Dominate mechanism | Kinetic | Diffusion |
|---|---|---|
| Isolated Line | 365 nm | 373 nm |
| Nested Lines | 350 nm | 342 nm |
| Simulated Isolated - Nested | +15 nm | +31 nm |
| Experimental Isolated - Nested | 0 to +20 nm | 0 to -350 nm |

The simulated results show the isolated line to be larger than the nested features for both the kinetic and diffusion mechanistic regions, with the higher developer selectivity and mth parameters yielding the larger bias. The bias in the kinetic region is consistant and of the same order of magnitude with the experimental data but not true for the diffusion controlled region. Varying the diffusion length arbitrarily until a fit for the diffusion controlled region is possible but not important to this current discussion. What is important is that that diffusion dominates the iso, nested feature bias above the inflection point, where there is a wide divergence between experiment and simulation, and that it does not significantly impact the bias at temperatures below the inflection. One explanation for this is that the inflection between the catalytic regions corresponds to the glass transistion temperature, $T_g$, of the exposed resist. Below the $T_g$, the acid mobility is hindered by a semi-rigid resist matrix. Above the $T_g$, the rigidness is gone and the acid is free to roam randomly through the resist. The affect that diffusion has on the iso, nested bias has to do with how the latent images of these two feature types change during the post exposure bake. Nested lines diffuse to some average acid concentration of the exposed and less exposed regions of the line, spaces. Isolated lines do the same thing. However, because of no close neigboring dark feature and because of a higher acid gradient to begin with, the isolated lines have both a larger acid gradient change and larger acid concentration than the nested lines do during the post exposure bake.

Further, refinement of the parameters extracted from the R(E,z) converter is accomplished by comparing the results of lithographic simulations using the range of parameter values from Table 2 against simulations using the R(E,z) data for a specific thermal dose and by, also, comparing the simulated to experimental imaging results. PROLITH/2 version 4.1a was used for the lithography simulations. To do this, the thermodynamic and development parameters derived from the R(E,z) to R(m,z) conversion are input into the simulator. The simulations are further constrained by using a sizing dose, $E_{SIZE}$, from a lithography study using the same lot of resist and one of the processes that was used to get the DRM data. The $E_{SIZE}$ from this study equaled 39.4mJ•cm$^{-2}$ for a 90°C for 90s thermal dose for 0.35μm clustered lines imaged with a 0.53NA/0.74σ/248.37nm GCA XLS stepper. Incidentally, this dose is in good agreement with the simulation result of 38.2mJ•cm$^{-2}$ for the same feature that was arrived at by using the 90°C for 90s PEB



Downloaded From: http://proceedings.spiedigitallibrary.org/ on 06/02/2014 Terms of Use: http://spiedl.org/terms

R(E,z) data set as the data base for the PROLITH/2 lithography engine[3]. Then using these parameters, nested multiple runs were made varying each of the parameters within there range of finite values allowed by the R(E,z) converter. This is repeated until the simualted values converged with the results of the based R(E,z) simulation.

## Conclusion

A method for converting rate versus exposure data to rate versus the relative remaining blocked sites on the resin was demonstrated. The model is based on kinetic and thermodynamic considerations of the photo and thermal dose given the resist during the imaging process. The current model includes an acid loss function that based on the low activation energy for the loss suggests that the acid is in equilibrium with other moieties in the resist. $R^2$ values in excess of 0.9 have been achieved using in the spread sheet analysis, but there is still considerable possibility for improvement by adding the effects of diffusion into the analysis and by using measurable parameters like $[M]_0$ in the analysis. To improve the fit within a given temperature range the data set used for this work was subdivided into temperature regions where good convergence was possible for each data subset. Using the current model, two distinct R(m,z) responses were found for the kinetically controlled low temperature and diffusion controlled high temperature regions of the XP-9402 resist. Using the parameters for the two regions simulations show agreement with experimental data for the kinetically controlled region but not for the diffusion controlled region. The disagreement with the high temperature region is because diffusion has not been considered in the current R(E,z) to R(m,z) converter.

---

[1] Shipley data generated by Mark Deneson.
[2] J. S. Petersen, T. H. Fedynyshyn, J. W. Thackeray, P. Freeman, D. A. Miller, "Design Issues for Making a Robust 248nm Acid Catlayzed Positive Photoresist", MicroProcess Conference'94, Hsinchu, Republic of China, 1994.
[3] FINLE Technologies, Inc., Austin, Texas, 78716



Downloaded From: http://proceedings.spiedigitallibrary.org/ on 06/02/2014 Terms of Use: http://spiedl.org/terms